

Original Article

Functional trait thermal acclimation differs across three species of mid-Atlantic harmful algae

Nayani K. Vidyarthna, Erin Papke, Kathryn J. Coyne, Jonathan H. Cohen, Mark E. Warner*

School of Marine Science and Policy, University of Delaware, Lewes, DE 19958, United States

ARTICLE INFO

Keywords:

Harmful algae
Climate change
Thermal optima
Photophysiology
Hemolytic activity
RT Fish gill cell toxicity

ABSTRACT

Characterizing the thermal niche of harmful algae is crucial for understanding and projecting the effects of future climate change on harmful algal blooms. The effects of 6 different temperatures (18–32 °C) on the growth, photophysiology, and toxicity were examined in the dinoflagellate *Karlodinium veneficum*, and the raphidophytes, *Heterosigma akashiwo* and *Chattonella subsalsa* from the Delaware Inland Bays (DIB). *K. veneficum* and *H. akashiwo* had skewed unimodal growth patterns, with temperature optima (T_{opt}) at 28.6 and 27.3 °C respectively and an upper thermal niche limit of 32 °C. In contrast, *C. subsalsa* growth increased linearly with temperature, suggesting T_{opt} and upper thermal boundaries >32 °C. *K. veneficum* photosystem II (PSII) photochemical efficiency remained stable across all temperatures, while *H. akashiwo* PSII efficiency declined at higher temperature and *C. subsalsa* was susceptible to low temperature (~18 °C) photoinactivation. Cell toxicity thermal response was species-specific such that *K. veneficum* toxicity increased with temperature above T_{opt} . Raphidophyte toxicity peaked at 25–28 °C and was in close agreement with T_{opt} for growth in *H. akashiwo* but below *C. subsalsa* maximal growth. The mode of toxicity was markedly different between the dinoflagellate and the raphidophytes such that *K. veneficum* had greater hemolytic activity while the raphidophytes had pronounced fish gill cell toxicity. These results and patterns of natural abundance for these algae in the DIB suggest that continued ocean warming may contribute to *C. subsalsa* bloom formation while possibly promoting highly toxic blooms of *K. veneficum*.

1. Introduction

Marine phytoplankton are responsible for nearly 50% of global primary productivity, and for approximately 98% of the ocean's primary productivity and the majority of biogeochemical cycling (Falkowski et al., 1998; Field et al., 1998). A small proportion of this phytoplankton community consists of harmful algal (HA) species, that are capable of producing high biomass and often mono-specific blooms with significant adverse effects on their ecosystems. Some harmful algae produce toxins which pass through the food web and cause fish and shellfish kills and human health effects (Anderson et al., 2012; Berdalet et al., 2016). While harmful algal blooms (abbreviated as HABs hereafter) are a natural phenomenon, the past few decades have witnessed a significant increase in their frequency, intensity and geographic range (Hallegraeff, 2010; Anderson et al., 2012). This increase is attributed in part to the effects of a changing climate, such as increased sea surface temperature, ocean acidification, and stratification (Hallegraeff, 2010; Wells et al., 2015; Gobler et al., 2017; Trainer et al., 2019).

Global temperature has already increased in measurable levels. Over 1971–2010, the upper 75 m of the ocean has warmed by 0.11 °C per decade and will continue to warm during the 21st century with a projected global surface temperature increase by >1.5 °C (IPCC, 2013). Temperature directly and indirectly influences phytoplankton physiology (Raven and Geider, 1988; Boyd et al., 2013; Baker et al., 2016, 2018), and is a major driver of phytoplankton biogeographic species boundaries (Thomas et al., 2012; Litchman et al., 2015), and projected warming could have significant effects on the ecophysiology and biogeography of many HAB species. Indeed, ocean warming has been recognized as a major environmental catalyst for the apparent increase of HABs (Paerl and Huisman, 2009; Tester et al., 2010; Gobler et al., 2017; Brandenburg et al., 2019). Higher temperature increases the growth of warm-water HAB species (e.g. *Gambierdiscus* spp, Tester et al., 2010; Kibler et al., 2012), induces greater cyst germination; e.g. *Chattonella* sp. (Yamaguchi et al., 2010), widens the temporal window for bloom formation (Moore et al., 2008; Gobler et al., 2017), increases the potential for HAB proliferation at higher latitudes (Brandenburg et al., 2019) and alters critical metabolic processes such as toxin production

* Corresponding author.

E-mail address: mwarner@udel.edu (M.E. Warner).

(Granéli et al., 2011; Ou et al., 2017; Aquino-Cruz et al., 2018; Basti et al., 2018). The thermal response, however, is fundamentally dependent on each species' thermal niche, which is characterized by lower and upper thermal boundaries and an optimum temperature at which growth (or other trait values) is maximized.

As local temperatures change or exceed these boundaries, phytoplankton respond via phenotypic plasticity, species sorting, genetic adaptation or by a combination of these processes (Litchman et al., 2012). Therefore, defining the thermal niche for HAB species is crucial for understanding and predicting the effects of future climate change on these globally important algae (Hallegraeff, 2010). In order to better understand how specific algal strains may respond to future warming, the present study determined the properties of the thermal niche for growth, photophysiology and toxicity of three major HAB forming species, *Karlodinium veneficum*, *Heterosigma akashiwo* and *Chattonella subsalsa*, commonly found in shallow mid-Atlantic coastal waters of the United States such as the Delaware Inland Bays (DIB) (Coyno et al., 2005; Handy et al., 2005, 2008; Demir et al., 2008; Zhang et al., 2006).

K. veneficum is a toxic, mixotrophic dinoflagellate that forms blooms associated with fish kills in estuarine and coastal waters around the world (Adolf et al., 2006, 2008, 2016; Zhou et al., 2011; Place et al., 2012). It produces a suite of toxic compounds known as karlotoxins (abbreviated as KmTx) with cytotoxic, ichthyotoxic and hemolytic properties (Deeds et al., 2002; Fu et al., 2010; Mooney et al., 2010; Place et al., 2012; Cai et al., 2016). These toxins also serve as grazer deterrents and allelochemicals and therefore affect a wide range of organisms including protists, zooplankton, shellfish and fish (Adolf et al., 2007; Waggett et al., 2008; Lin et al., 2017; Binzer et al., 2018). The type(s) of KmTx present in *K. veneficum* depends on the specific strain and their toxin potency is often modulated by the environmental conditions (Bachvaroff et al., 2009; Fu et al., 2010; Mooney et al., 2010; Place et al., 2012; Cai et al., 2016). The *K. veneficum* strain used in this study (CCMP 2936) is known to produce KmTx-1 and KmTx-2 and has shown hemolytic activity (Fu et al., 2010). Because of its wide range of activity and variation, cell toxicity is perhaps the most studied trait of this species (Adolf et al., 2007, 2008, 2016; Deeds et al., 2002; Mooney et al., 2010; Fu et al., 2010; Dorantes-Aranda et al., 2011). In general, *K. veneficum* physiology (growth, toxicity, mixotrophy, photochemistry) is known to be influenced by temperature, availability of inorganic nutrients and prey, light intensity, and dissolved inorganic carbon (Adolf et al., 2007, 2008; Fu et al., 2010; Tilney et al., 2014; Lin et al., 2017, 2018a, 2018b). While their physiological responses (e.g. growth and/or cell toxicity) are highly strain-specific, *K. veneficum* grows over a broad range of temperature (7–30 °C) and salinities (5–30) (Nielsen, 1996; Adolf et al., 2009; Li et al., 2015).

H. akashiwo and *C. subsalsa* are marine bloom-forming mixotrophic raphidophytes that are also associated with massive fish kills in several areas (Jeong et al., 2010; de Boer et al., 2012; Cho et al., 2016). Even though the fish killing mechanisms by raphidophytes are often linked to the production of reactive oxygen species (ROS) and/or the neurotoxin-like compounds (Portune et al., 2010; Cho et al., 2016) their toxin profiles and specific modes of toxicity are not well established. Both *H. akashiwo* and *C. subsalsa* are found naturally in a wide range of temperatures (5–33 and 17–33 °C, respectively) and salinities (1–35 and 6–36, respectively) (Zhang et al., 2006; Imai and Yamaguchi, 2012), which is likely due to genetic variation and hence population specific (i.e., clonal) differences within each of these species.

While temperature is not always the main environmental driver for bloom formation, it can play a critical proximate role. *K. veneficum* blooms are promoted by the availability of nutrients and protist prey (Adolf et al., 2008; Li et al., 2015; Lin et al., 2018b), yet most blooms, such as those recorded in Chesapeake Bay, occur when the water temperature is above 20 °C, even though they can survive at temperatures as low as ~6 °C (Li et al., 2015; UD citizen monitoring program). For raphidophytes, successful cyst germination is a crucial factor for

bloom initiation (Imai and Yamaguchi, 2012). Germination is temperature sensitive, and vegetative cells germinated at higher temperatures often display higher survival (Shikata et al., 2007, 2008; Portune et al., 2009; Yamaguchi et al., 2010). Temperature also alters HAB toxin production (Granéli and Flynn, 2006; Granéli et al., 2011; Ou et al., 2017; Aquino-Cruz et al., 2018), and in many cases, provides a competitive advantage and increased survival, even when conditions are not optimal for their growth (Tillmann and John, 2002; Granéli and Flynn, 2006; Glibert, 2016). Hence, the thermal optima for toxin production may not necessarily correspond to the growth optima, and this is also true for other functional traits such as those related to photosynthesis (Ou et al., 2017; Aquino-Cruz et al., 2018). For example, higher temperature (30 °C) led to a decline in growth and photochemical efficiency of the toxic benthic dinoflagellate *Prorocentrum lima* but still led to higher okadaic acid toxicity (Aquino-Cruz et al., 2018).

As population growth is a critical outcome, especially with concern to HABs, understanding the thermal response of other key physiological traits provide better insight into the autecology of HAB species in response to projected climate change. We hypothesized that, with regards to cellular growth, each alga would display a unimodal thermal response curve, and that the thermal optima (T_{opt}) derived from these curves would be similar across all three species. Previous studies with the same isolate of *H. akashiwo* and *C. subsalsa* from the DIB (Zhang et al., 2006) as well as a different isolate of *K. veneficum* from the Chesapeake Bay (Adolf et al., 2009) noted roughly equivalent growth across a broad temperature range (~16–28 °C), but neither study was specifically designed to test thermal acclimation. We further hypothesized that the response of functional traits related to photosynthesis for each species would be less temperature dependent when compared to patterns of cellular growth, however, cellular toxicity would closely follow a pattern similar to the growth thermal optima for each alga.

2. Materials and methods

2.1. Phytoplankton cultures and experimental design

Non-axenic cultures of the dinoflagellate *Karlodinium veneficum*, and the raphidophytes *Heterosigma akashiwo*, and *Chattonella subsalsa* were previously collected from the Delaware Inland Bays (CCMP 2936, CCMP 2393 and CCMP 2191 respectively; National Center for Marine Algae and Microbiota, Bigelow, USA). Initial replicate ($n = 4$) batch cultures were grown in modified f/2 media (320 μM NO_3^- and 20 μM PO_4^{3-} , Guillard and Ryther, 1962) at 25 °C with light intensity of 100 $\mu\text{mol photons m}^{-2} \text{s}^{-1}$ (cool white fluorescent bulbs) on a 12:12 h light:dark cycle. The culture medium was prepared with natural seawater diluted to a salinity of 20, followed by filtration (Whatman Polycap 75 TC, 0.2 μm nominal pore) and autoclaved. All experiments were conducted in replicate ($n = 4$) 500 mL Erlenmeyer flasks with initial culture volumes of 300 mL. All experiments were started with exponentially growing cultures under optically thin conditions with in vivo fluorescence ranging from 2 to 10 relative fluorescence units. Experiments were conducted at six different temperatures (18, 22, 25, 28, 30 and 32 °C), while all other conditions were maintained as described above. Cultures were initially shifted from 25 °C to either 22 or 28 °C by slowly ramping to the target temperature at a rate of 0.5 °C day^{-1} in temperature-controlled incubators (Percival Scientific). Once reaching the target temperature, cultures were re-inoculated into the fresh media and were further acclimated for at least 4 generations before further measurements after another 7–10 days of subsequent growth. Remaining cultures at the new low/high temperature were subsequently shifted to the next lower/higher temperature respectively, using the same rate of temperature ramping and acclimation period until the next target temperatures were reached.

Algal growth was followed by measuring in vivo chlorophyll *a* (chl *a*) fluorescence (10 AU; Turner Designs, USA) of sub samples (5 mL)

withdrawn from each culture flask daily for 7–10 days. Specific growth rates (μ , day^{-1}) were calculated based on the fluorescence during the exponential growth phase using the following formula:

$$\mu = \frac{(\ln N_2 - \ln N_1)}{(t_2 - t_1)} \quad (1)$$

where N_1 and N_2 are in vivo chl *a* fluorescence at time t_1 and t_2 .

Experiments were terminated when cultures reached late exponential phase growth, and samples were collected for analyses of final cell density, chl *a* concentration, active chl *a* fluorescence, cellular carbon, nitrogen and toxicity.

2.2. Cell densities

Sub samples (1 mL) were preserved with glutaraldehyde (final concentration 1% v/v) and were manually counted using a 0.1 mm Neubauer or a 0.2 mm Fuchs-Rosenthal hemocytometer using a light microscope at 100x magnification.

2.3. Chlorophyll *a* content

2 mL sub samples from each replicate were centrifuged at $3380 \times g$ for 5 min at 4 °C. Supernatants were discarded and the cell pellets were extracted in 2 mL of 90% acetone for 2–3 h in the dark at -20 °C. Acetone extracts were centrifuged ($3380 \times g$, 5 min at 4 °C) to remove the cell debris and chl *a* was measured fluorometrically (10 AU; Turner Designs, USA), using the non-acidification method of Welschmeyer (1994).

2.4. Algal photophysiology

Photochemistry of late exponential phase cultures was assessed by fast repetition rate fluorometry (FRRf) with a FASTtrack II fluorometer connected to a FASTact light and temperature control assembly connected to a constant temperature water bath set to each growth temperature (Chelsea Instruments, UK). Prior to measurements, *K. veneticum* samples were dark acclimated for 15 min and, to avoid dark-induced reduction of the plastoquinone pool, raphidophyte samples were held under low light ($c. 5 \mu\text{mol photons m}^{-2} \text{s}^{-1}$) prior to dark acclimation for 3 min (Hennige et al., 2013). The single turnover fluorescence protocol consisted of 100 1 μs flashlets at $\sim 1\text{-}\mu\text{s}$ intervals provided by a bank of blue LEDs (peak excitation 450 nm, 200 μs total induction time), followed by 50 flashlets spaced at 49 μs intervals to allow relaxation and re-oxidation of the PSII reaction center. Measurements were recorded from the average of 15–30 acquisitions at 100 ms intervals. In order to record photochemical activity in the light activated state similar to the growth light level, samples were exposed to a bank of white LEDs set to 104 $\mu\text{mol photons m}^{-2} \text{s}^{-1}$ for 3 min prior to another round of fluorescence induction measurements. Fluorescence data were fit in FASTpro software (v3.0, Chelsea Instruments) and used to calculate maximum quantum yield of photosystem II (F_v/F_m), the quantum yield of photosystem II in the light activated state (F_q'/F_m), and the functional absorption cross section of photosystem II in the dark and light (σ_{PSII} and $\sigma_{\text{PSII}'}$, respectively) (Cosgrove and Borowitzka, 2010).

2.5. Cellular carbon and nitrogen

Samples for cellular organic nitrogen and carbon were filtered onto 25 mm pre-combusted glass-fiber filters (2 h at 450 °C, GF/C, Whatman), dried at 60 °C for 24 h and then stored in a desiccator prior to analyses. Cellular carbon and nitrogen were then quantified with a CHN elemental analyzer (ECS 4010 Elemental combustion system; Costech Instruments, USA), with phenylalanine and EDTA used as standards.

2.6. Cellular toxicity

Cell toxicity was assessed by both a hemolytic toxicity assay and a Rainbow Trout (RT) fish gill cell toxicity (FGC) assay. Hereafter, hemolytic activity and FGC toxicity refers to the specific toxicities assessed with the hemolytic assay and FGC assay respectively while the term 'cell toxicity' collectively refers to both hemolytic activity and FGC toxicity, throughout the text.

50 mL-samples were withdrawn from each replicate algal flask and centrifuged at 5000 rpm for 5 min at 4 °C (Sorval RC-5B, USA). Cell pellets were extracted in 1–2 mL of methanol for 24 h in the dark and stored at -20 °C until further analyses. Hemolytic activity was measured in methanol extracts following previously published methods (Eschbach et al., 2001; Vidyarthna and Granéli, 2012) with some modifications. Briefly, methanol extracts were mixed in different ratios, ranging from 4% to 50%, with isotonic phosphate buffer (IPB) in 96-well microplates, after which 200 μL of a 5% rabbit blood cell suspension (IRI-050-K2 EDTA; Innovative Research, USA) in IPB was added and incubated for 1 h at 25 °C in continuous light ($\sim 100 \mu\text{mol photons m}^{-2} \text{s}^{-1}$). Standard curves were created by measuring the hemolytic activity of Saponin (S7900; Sigma Aldrich, USA) in IPB. Following incubation, plates were centrifuged at $1260 \times g$ for 5 min (Eppendorf, Centrifuge 5804), and 100 μL of supernatants were transferred into new 96-well plates and the absorbance was measured at 415 nm in a microplate reader (FLUO Star Omega; BMG LABTECH). Cellular hemolytic activity was calculated relative to saponin hemolytic activity and expressed as pg saponin equivalent cell⁻¹ (Vidyarthna and Granéli, 2012).

Toxicity by the RT fish gill cell line assay followed the methods of Dayeh et al. (2005), Dorantes-Aranda et al. (2011) and Ikeda et al. (2016). Cell pellets were extracted in MeOH as described above. Extracts were then evaporated under a flow of ultra-high purity nitrogen gas at 25 °C and then resuspended in filter sterilized (0.2 μm) L-15/ex media (Schirmer et al., 1997; Ikeda et al., 2016). Extracts were then vortexed and sonicated in a bath-type sonicator (Sonicor, USA) for 5 min and stored at -20 °C until further analyses. Sterile 96-well plates were seeded with a RT fish gill cell culture in complete Leibovits- L15 medium (L-15 supplemented with 10% Fetal Bovin Serum and 1% antibiotic and antimycotic solution) at a concentration of 1.5×10^5 cells mL^{-1} and were incubated for ~ 36 hrs at 18 °C. The L-15 medium was then replaced with sterile L-15/ex media and cells were incubated further for another 6–12 h in the same conditions (Ikeda et al., 2016). The gill cells were then exposed to a concentration series of each algal extract in L-15/ex for 6 hrs at 18 °C in the dark. These test solutions were then replaced by 5% Alamar Blue solution (DAL1025; Invitrogen, USA), incubated for 2 h at 18 °C in the dark, and the cell viability was determined by measuring fluorescence in a plate reader with excitation and emission filters of 544 nm and 590 nm, respectively (FLUO Star Omega; BMG LABTECH).

FGC percent mortality was calculated as:

$$\% \text{mortality} = \left[1 - \frac{(RFU_{\text{extract}} - RFU_{\text{pos. control}})}{(RFU_{\text{neg. control}} - RFU_{\text{pos. control}})} \right] \times 100 \quad (2)$$

where, RFU_{extract} is the fluorescence measured after exposing the gill cells to algal extracts, $RFU_{\text{pos. control}}$ is the fluorescence measured after exposure to a positive control (3% H_2O_2 , i.e., considered the 100% mortality) and $RFU_{\text{neg. control}}$ is the fluorescence measured from cells in L-15/ex alone and considered to represent 100% viability. Dose response curves were fit by a non-linear curve fit routine in GraphPad PRISM in order to calculate the algal cell density that caused 50% FGC mortality (EC_{50}).

In order to account for possible differences in algal cell size between the different species and different growth temperatures, hemolytic activity and FGC EC_{50} values were normalized to total cellular carbon and expressed as pg saponin equivalent pg C^{-1} and $\mu\text{g C mL}^{-1}$ respectively.

We were unable to quantify the toxicity of all algae grown at 18 °C as hemolytic activity and FGC toxicities were below the limits of detection. In addition, due to limited material for some species, toxicity samples were not collected at 32 °C.

2.7. Data analyses

Statistical analyses were performed using R statistical software (v 3.5.2; R Core Team 2018) or GraphPad Prism (v 8.0.0). The data were checked for normality with the Shapiro-Wilk test while homogeneity of the variances was assessed with the Bartlett test.

For *K. veneficum* and *H. akashiwo* growth vs. temperature curves were analyzed using the Sharpe-Schoolfield equation for high temperature inactivation (Schoolfield et al., 1981), by the following equation:

$$\mu(T) = \frac{\mu_{T_{ref}} \exp\left(\frac{E_a}{k} \left(\frac{1}{T_{ref}} - \frac{1}{T}\right)\right)}{1 + \exp\left(\frac{E_h}{k} \left(\frac{1}{T_h} - \frac{1}{T}\right)\right)} \quad (3)$$

where $\mu(T)$ is the growth rate (day^{-1}), k is Boltzmann's constant ($8.62 \times 10^{-5} \text{ eV K}^{-1}$), E_a is the activation energy (in electron volts, eV) that describes the increase of growth rate before the optimum temperature (T_{opt}), T is growth temperature in Kelvin (K), T_h is the temperature at which half of the enzymes become nonfunctional and therefore, the growth rate is at half maximum, E_h is the growth rate decline (deactivation energy) above T_h , and $\mu_{T_{ref}}$ is the growth rate at the starting reference temperature T_{ref} (25 °C). Eq. (3) yields a maximum growth rate at an optimum temperature (T_{opt}):

$$T_{opt} = \frac{E_h T_h}{E_h + k T_h \ln\left(\frac{E_h}{E_a} - 1\right)} \quad (4)$$

The temperature range at which the growth rates were positive (>0) was considered the thermal niche width (Baker et al., 2016). Data were fit to Eq. (3) using non-linear least square regression using the 'nls.multstart' package, with model optimization by the Akaike Information Criterion (AIC) score (Padfield and Matheson, 2018). Model confidence intervals were calculated by parametric bootstrapping (1000 replicates) using the 'bootstrap' function in the 'modelr' package in R (Wickham, 2019). These synthetic data were then fit to Eq. (3) to generate a new set of parameters for E_a , $\mu_{T_{ref}}$, E_h and T_h . T_{opt} at each bootstrap iteration was calculated using Eq. (4). 95% confidence intervals for each parameter were calculated by taking the range between the 2.5th and 97.5th quantiles. Residuals for each model fit were evaluated for a random normal distribution using the 'test.nlsResiduals' function of the 'nlstools' package in R (Baty et al., 2015). As growth vs. temperature patterns for *C. subsalsa* did not display a conventional thermal optimum curve, the Sharpe-Schoolfield model was not appropriate and instead data were compared by linear regression (GraphPad Prism, v 8.0.0).

Maximum growth rates, algal photophysiology (F_v/F_m , σ_{PSII}), cellular chl a , carbon and nitrogen, atomic ratios of C:N, and cell toxicities for each algal species at each temperature were statistically compared using one-way analysis of variance (ANOVA) followed by Tukey HSD post hoc tests in R. Results were considered significant at $\alpha = 0.05$.

3. Results

3.1. Growth rate

Both *K. veneficum* and *H. akashiwo* displayed skewed unimodal growth patterns with temperature, where growth peaked at a thermal optimum (T_{opt}) and then rapidly declined (Fig. 1A and B). Calculated T_{opt} for *K. veneficum* was 28.6 °C (95% CI: 28.44–28.58 °C), while T_{opt}

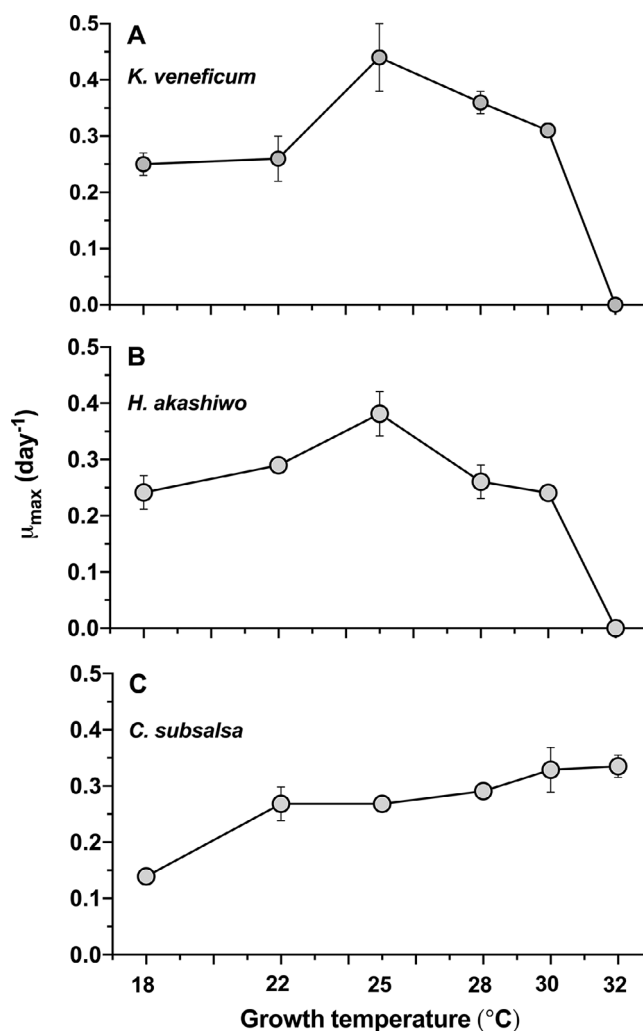


Fig. 1. Maximum growth rates (μ_{max} , day^{-1}) of *K. veneficum* (A), *H. akashiwo* (B) and *C. subsalsa* (C) at the six different temperatures. Errors denote the standard deviation of four replicates ($n = 4$).

for *H. akashiwo* was slightly lower at 27.3 °C (95% CI: 27.18–27.44 °C). Neither species grew at 32 °C and hence this temperature set the upper thermal limit under these experimental conditions for both species. While the lower limit for the thermal niche for these species could not be calculated, the data suggest that they were <18 °C.

In contrast, *C. subsalsa* growth increased linearly with increasing temperature ($p = 0.008$, $R^2 = 0.86$; Fig. 1C) with the lowest growth at 18 °C ($0.14 \pm 0.01 \text{ d}^{-1}$) (Tukey's HSD, $p < 0.001$ compared to all the other rates) and the highest growth at 28–32 °C ($0.29 - 0.33 \text{ d}^{-1}$). Growth rates at 28 °C were significantly higher when compared to μ_{max} at 18 °C (Tukey's HSD, $p < 0.001$), while the growth rates at 30 and 32 °C were significantly higher compared to growth at 22 and 25 °C as well (Tukey's HSD, $p < 0.05$ in both cases).

3.2. Algal photochemistry and chlorophyll a content

The maximum quantum yield of PSII (F_v/F_m) in *K. veneficum* remained unchanged across the entire temperature range (ANOVA, $p = 0.19$) (Fig. 2A). In contrast, both raphidophytes showed significant variation in F_v/F_m in response to temperature (ANOVA, $p < 0.001$ for both species, Fig. 2B and C). F_v/F_m of *H. akashiwo* was significantly greater at 25 °C as compared to all other temperatures (Tukey's HSD, $p < 0.001$), while there was no significant difference between values recorded at 18, 22 and 28 °C (Tukey's HSD, $p > 0.05$) (Fig. 2B).

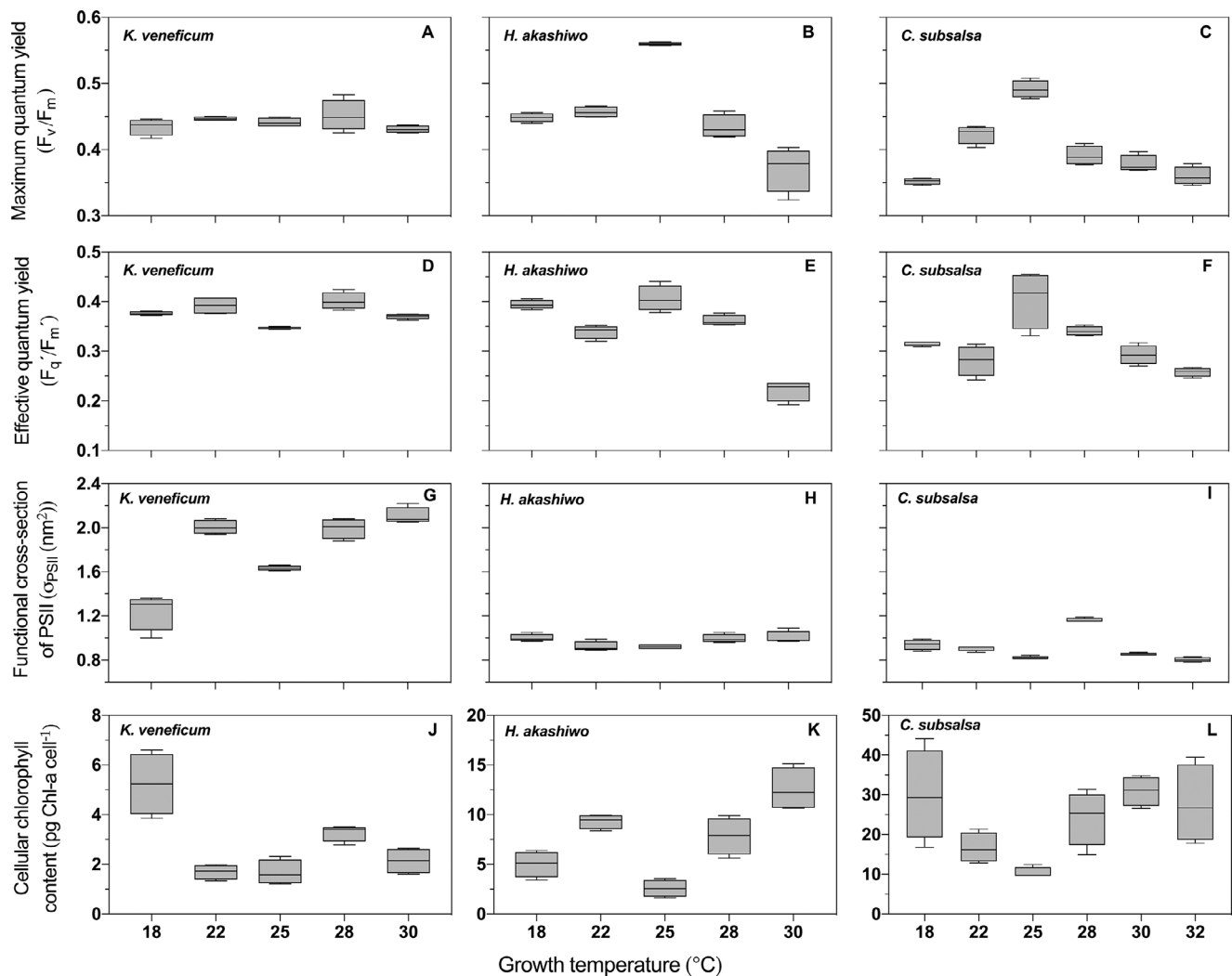


Fig. 2. Thermal response of algal photochemistry and chlorophyll *a* content of *K. veneficum* (A, D, G, J), *H. akashiwo* (B, E, H, K) and *C. subsalsa* (C, F, I, L) at the six different temperatures. Presented for each species are: Maximum photochemical efficiency of photosystem II (F_v/F_m) (A, B and C); effective light acclimated photochemical efficiency of PSII (F_q'/F_m') (D, E and F); functional PSII absorption cross section (σ_{PSII}) (nm^2 , G, H and I) and Chl-*a* (pg cell^{-1} , J, K and L), ($n = 4$).

However, F_v/F_m was significantly lower at 30 °C when compared to the other temperatures (Tukey's HSD, $p < 0.001$). Similar to *H. akashiwo*, F_v/F_m for *C. subsalsa* was significantly higher at 25 °C than at all other temperatures (Tukey's HSD, $p < 0.001$) (Fig. 2C). Compared to values recorded at 22, 25 and 28 °C, F_v/F_m declined significantly at both the low and high temperature extremes (18 and 32 °C, Tukey's HSD, $p < 0.03$), and in marked contrast to *K. veneficum* and *H. akashiwo*, there was a greater drop in F_v/F_m as temperatures lowered from 25 to 18 °C.

The effective quantum yield of PSII in the light acclimated state (F_q'/F_m') of *K. veneficum* ranged between 0.35 and 0.40 (Fig. 2D) and exhibited a temperature trend similar to that noted for F_v/F_m . F_q'/F_m' of *H. akashiwo* ranged between 0.22 and 0.41 (Fig. 2E), and the highest values were at 25 °C (Tukey's HSD, $p < 0.02$ compared to 22, 28 and 30 °C). Likewise, F_q'/F_m' dropped to a greater degree at 30 °C when compared to F_v/F_m (Tukey's HSD, $p < 0.001$ for all the other temperatures). While the highest F_q'/F_m' for *C. subsalsa* was recorded at 25 °C (Tukey's HSD, $p < 0.004$ compared to 18, 28, 30 and 32 °C), it did not show a clear rapid increase as found for F_v/F_m at 18–25 °C (Fig. 2F). However, F_q'/F_m' decreased significantly at 28–32 °C (Tukey's HSD, $p < 0.05$ compared to 25 °C), while the lowest F_q'/F_m' values were found at the low (18–22 °C) and high (30–32 °C) ends of the tested temperature range.

In contrast to the patterns in PSII photochemical efficiency, the functional absorption cross section of photosystem II (σ_{PSII}) of *K.*

veneficum significantly increased with temperature (Fig. 2G) resulting in a 1.6-fold higher (61% increase) σ_{PSII} at 22 °C compared to that at 18 °C, and σ_{PSII} at 18 °C was significantly lower than at all the other temperatures (Tukey's HSD, $p < 0.001$). However, σ_{PSII} of both raphidophytes varied minimally across the temperature range (Fig. 2H and I, ANOVA, $p > 0.05$).

For all algae, cellular chl *a* did not show a clear trend with temperature (Fig. 2J–L), but some species-specific differences were evident. *K. veneficum* had significantly higher chl *a* content at 18 °C (Tukey's HSD, $p < 0.005$ for all other temperatures), while values at higher temperatures varied minimally, except for a slight yet significant increase in chl *a* at 28 °C (when compared to levels at 22 and 25 °C, Tukey's HSD, $p < 0.04$ for both cases). *H. akashiwo* grown at 30 °C had significantly higher chl *a* content (Tukey's HSD, $p < 0.05$ for all other temperatures), but lacked a clear trend with temperature. Similarly, cellular chlorophyll in *C. subsalsa*, was largely invariant across the temperature range except at 25 °C, which was significantly lower compared to levels at 18, 30 and 32 °C (Tukey's HSD, $p < 0.03$).

3.3. Cellular carbon and nitrogen

Growth temperature also affected the stoichiometry of cellular carbon (C) and nitrogen (N) (Supplementary Table 1). Of all three species, *H. akashiwo* had the least variation in C and N cellular quotas

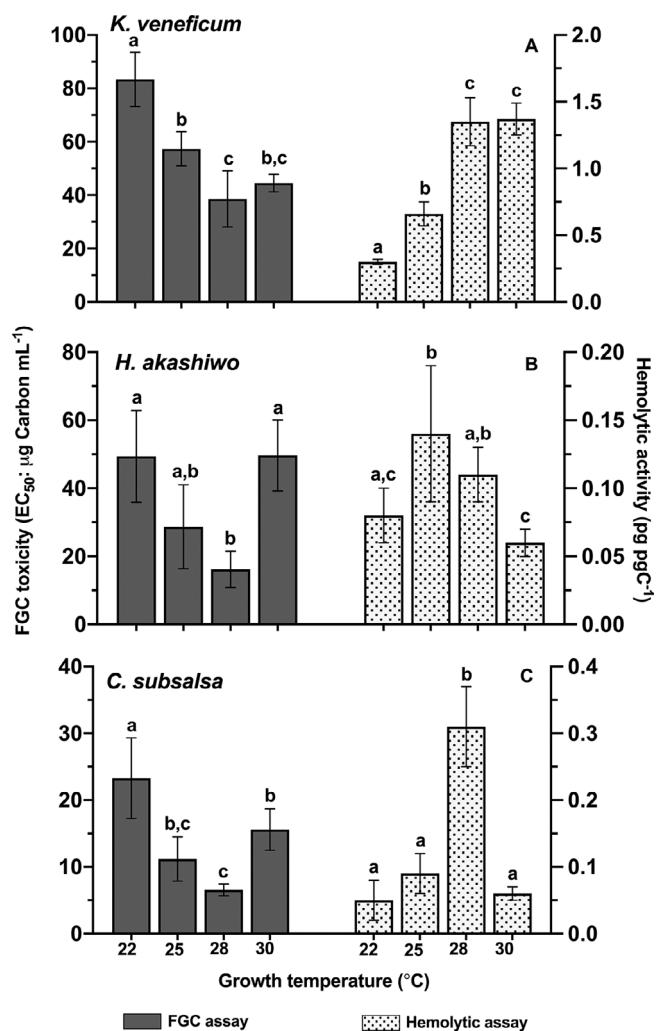


Fig. 3. RT fish gill cell toxicity (EC_{50} ; $\mu\text{g Carbon mL}^{-1}$ - Left Y axes) and the hemolytic activity (pg C^{-1} - Right Y axes) of *K. veneficum* (A), *H. akashiwo* (B) and *C. subsalsa* (C) at four different temperatures. Errors denote the standard deviations of four replicates ($n = 4$). Letters above the bars indicate significant intraspecific differences between treatments (Tukey's HSD, $p < 0.05$). Note that lower EC_{50} values for the FGC assay equate to higher toxicity.

across all the temperatures (2.5 and 1.8-fold, for C and N, respectively). In contrast, C and N quotas for *K. veneficum* varied across all temperatures as much as 2.5 and 7.4-fold, respectively, with the highest C and N contents at 18 °C (Tukey's HSD, $p < 0.001$ for all other temperatures). *C. subsalsa* showed higher variations for both C and N contents across all the temperatures (7.8 and 7.4 fold, respectively) showing the highest C and N contents at 18 °C, and the lowest at 28 °C. Atomic ratios of C:N varied in the range of 6.4–10.6 for *H. akashiwo* and 6.9–10.3 for *C. subsalsa* across all the temperatures (Supplementary Table 1). However, it varied from 2.7 to 9.6 for *K. veneficum* and this was driven by the significantly low C:N ratio noted at 18 °C (2.68 ± 0.29 ; Tukey's HSD, $p < 0.001$ for all other temperatures).

3.4. Cell toxicity

Cell toxicities (by both hemolytic activity and FGC toxicity) changed significantly with growth temperature of all three species (Fig. 3A–C; ANOVA, $p < 0.001$). There was a significant increase in cell toxicity with temperature for *K. veneficum*, and in particular for hemolytic activity (Fig. 3A). The highest hemolytic activity for *K. veneficum* was recorded at both 28 and 30 °C compared to those at 25 and 22 °C (Tukey's HSD $p < 0.001$), while the FGC toxicity showed similar

toxicity levels at 25–30 °C (Tukey's HSD $p < 0.003$), although the FGC toxicity at 28 °C was significantly higher than that at 25 °C (Tukey's HSD $p = 0.03$). *K. veneficum* grown at 22 °C exhibited the lowest hemolytic activity ($0.30 \pm 0.02 \text{ pgC}^{-1}$) and the lowest FGC (EC_{50} : $83.4 \pm 10.2 \mu\text{gC mL}^{-1}$) toxicities (Tukey's HSD $p < 0.004$ and $p < 0.003$ for hemolytic and FGC assays respectively).

Unlike *K. veneficum*, cell toxicities of *H. akashiwo* and *C. subsalsa* increased with the temperature, peaked at 25–28 °C and then decreased with a further increase of temperature up to 30 °C (Fig. 3B and C). For *H. akashiwo*, while toxicity was the highest (and statistically the same) between 25 and 28 °C, the two assays did not entirely agree with each other across the whole temperature range. Specifically, there was no difference in toxicity between 22, 25 and 30 °C by the FGC assay, while toxicity by the hemolytic assay indicated no statistical difference between 22 and 28 °C (Fig. 3B). The hemolytic activity at 25 °C was significantly higher compared to activity at 22 and 30 °C (Tukey's HSD $p < 0.007$ for both cases). For *C. subsalsa* toxicity by hemolytic assay showed a significant increase at 28 °C (Tukey's HSD $p < 0.001$ for all other temperatures) (Fig. 3C), with no statistical difference in hemolytic activity between 22, 25 and 30 °C. However, *C. subsalsa* FGC toxicity increased both at 25 and 28 °C (Tukey's HSD $p < 0.02$ for 28 °C compared to 22 and 30 °C, and $p = 0.003$ for 25 °C compared to 22 °C).

When comparing peak hemolytic activity and FGC toxicity across the different algal species, significant but contrasting interspecific differences were found (ANOVA, $p < 0.001$ and $p = 0.001$ for hemolytic and FGC assays, respectively). In terms of hemolytic activity, *K. veneficum* was the most toxic, and had ~10- and 4.4-fold higher hemolytic activities compared to the peak activities of *H. akashiwo* and *C. subsalsa* (note the scale difference between Fig. 3A–C; Tukey's HSD $p < 0.001$ for both cases). However, when comparing peak FGC toxicities, the two raphidophytes were more toxic (lower EC_{50} values) than *K. veneficum* (Tukey's HSD $p < 0.006$ in both cases).

4. Discussion

Phenotypic plasticity is a fundamental response of many functional traits to environmental change. Trait expression varied substantially across different temperatures and/or between different species, indicating that each species potentially has mechanism(s) to respond to ocean warming but not to the same capacity. Thermal optima ($Topt$) for growth rates did not necessarily reflect the $Topt$ of other functional traits of the same species, showing the high level of variation and the magnitude of plasticity between different traits of the same species. Likewise, not all responses had clear $Topt$ patterns across the temperature range examined.

4.1. Phenotypic plasticity of growth

When considering specific cellular traits that may lead to local dominance, net population growth rate represents a proxy for fitness (Geider et al., 2009). Given the unexpected linear pattern of increased growth with elevated temperature, *C. subsalsa* was the most resilient algal strain to warming when compared to the other species. In agreement with thermal performance curves (TPCs) for growth of many autotrophic phytoplankton (Boyd et al., 2013; Baker et al., 2016, 2018; Stawiariski et al., 2016; Demory et al., 2019), *K. veneficum* and *H. akashiwo* had typical skewed unimodal TPCs for growth. Growth above $Topt$ declined sharply in both species with significantly higher deactivation energies (E_d : 20.3 and 19.4 eV for *K. veneficum* and *H. akashiwo*, respectively) as compared to their activation energies (E_a : 0.35 and 0.30 eV for *K. veneficum* and *H. akashiwo*, respectively). Such growth declines at the highest temperatures may be linked to dysfunction of key metabolic enzymes and are often accompanied by loss of thylakoid membrane integrity and damage to the photosynthetic electron transport chain (Salvucci and Crafts-Brandner, 2004). In contrast, temperatures well below $Topt$, can lead to lower membrane fluidity and reduced

substrate affinity for active transport processes (e.g. nitrate), and growth (reviewed in Nedwell, 1999).

Phytoplankton thermal responses are often strain-specific (Boyd et al., 2013). Our *K. veneticum* strain isolated from DIB (CCMP 2936) had a higher *Topt*, and a larger upper thermal boundary than other previously studied *K. veneticum* strains. For example, *K. veneticum* (CCMP 1975) originating from the Chesapeake Bay had a similar thermal window as noted here (<12–28 °C), but a *Topt* closer to 20 °C (Lin et al., 2018a). Nielsen (1996) also noted optimal *K. veneticum* growth at 20–24 °C (but the upper thermal boundary was not established). Interestingly, both the Chesapeake Bay and Delaware strains exhibited limited declines in growth at sub-optimal temperatures below ~25 °C, hence mid Atlantic *K. veneticum* populations are able to survive temperatures well below 18 °C. In fact, Nielsen (1996) reported *K. veneticum* growth at temperatures as low as 7 °C, with $\mu > 0.1 \text{ day}^{-1}$. While the availability of nutrients and prey are considered major drivers promoting many *K. veneticum* blooms (J.E. Adolf et al., 2008; Li et al., 2015; Lin et al., 2018b), water temperature and cell abundance were positively correlated (Li et al., 2015). For example, ~80% of *K. veneticum* blooms in the Chesapeake developed when water temperatures were 20.7–30 °C (Li et al., 2015), and 30 °C sets the upper thermal boundary for the growth of our local *K. veneticum* isolate as well. Naturally, temperature may not necessarily be the proximate driver in all cases and other factors related to bloom seasonality (e.g., precipitation or water column stability) could be more important.

An earlier study with the same strains of *H. akashiwo* and *C. subsalsa* noted relatively constant growth from 20 to 30 °C (Zhang et al., 2006) as opposed to the unimodal (*H. akashiwo*) and linear (*C. subsalsa*) growth trends noted here. The marginal change in growth across temperature noted by Zhang et al., (2006) may have been due to differences in acclimation time to each temperature (not reported in their study) as well as other culture conditions (e.g., light and starting cell density). However, in agreement with our study, Fu et al., (2008) noted significantly higher growth for *H. akashiwo* at 24 °C when compared to 20 °C. Critically, maximum growth (μ_{max}) varies considerably across different experimental designs, while *Topt* is a more robust trait for examining thermal growth patterns between studies (Boyd et al., 2013). Despite these differences, there is a common trend across many *H. akashiwo* strains where growth tends to increase with temperature from 14 to 27 °C (Ikeda et al., 2016; Martínez et al., 2010).

Higher temperatures are also critical for rapid cyst germination and higher survival of germinated cells (Shikata et al., 2007; T. 2008). While natural *H. akashiwo* distributions tend to fall within a broad temperature range (5–33 °C), most blooms occur within a more narrow range of approximately 5–6 °C, such as 18–24 °C in Bay of Biscay, Spain (Martínez et al., 2010) or 21–26 °C in Hakata Bay, Japan (Shikata et al., 2008). Further, contrasting ecotypes of *H. akashiwo* with differing growth and competitive abilities within the same geographic region are also affected by several factors beyond temperature, such as light and salinity (Martínez et al., 2010; Fredrickson et al., 2011; Strom et al., 2013). While a single strain is not representative of the entire *H. akashiwo* population, many studies support our findings of an upper thermal boundary near 32 °C and *Topt* of ~27 °C.

The *C. subsalsa* growth response from 18 to 32 °C was strikingly different from that of most other phytoplankton published to date. Many *Chattonella* species have optimal growth temperatures ranging from 25 to 30 °C, with a marked drop in growth >30 °C (reviewed in Imai and Yamaguchi, 2012). However, similar to our observations, higher temperature preferences were noted for three strains of *C. ovata* from Hiroshima Bay, Japan where higher growth rates (>1.0 divisions d^{-1}) were found up to 32.5 °C (Yamaguchi et al., 2010). In addition, we have also found that the DIB *C. subsalsa* strain survives short term (<6 h.) temperature shocks up to 40 °C (personal observation). Similar to *H. akashiwo*, higher temperatures also promoted cyst germination in *Chattonella ovata*, with an optimum near 30 °C (Yamaguchi et al., 2010). This temperature-growth relationship for cell growth and possibly cyst

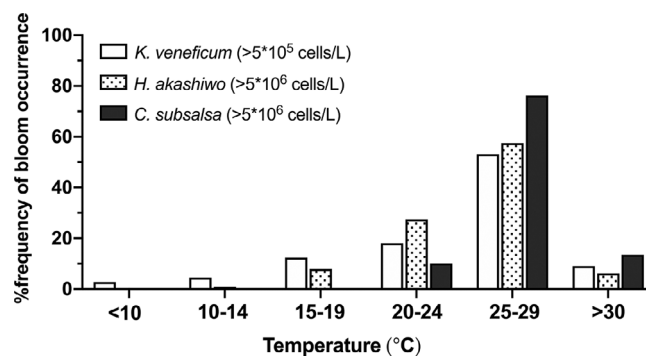


Fig. 4. Percent frequency of bloom occurrence with water temperature collected 2002–2018 for *K. veneticum*, *H. akashiwo* and *C. subsalsa* in the Delaware Inland Bays. Data were obtained from the UD citizen monitoring program (<https://www.citizen-monitoring.udel.edu/>).

germination may explain why this alga tends to bloom at slightly warmer temperatures (>17 and >24 °C, respectively) than *H. akashiwo* in the Delaware Inland Bays.

We further examined the relationship between temperature and bloom occurrence of these three HAB species in situ, by analyzing the cell density vs. water temperature data collected by a local citizen phytoplankton monitoring program from 2002 to 2018 (<https://www.citizen-monitoring.udel.edu/>). Records exceeding the respective bloom thresholds ($\geq 5 \cdot 10^5 \text{ cells L}^{-1}$ for *K. veneticum* (Li et al., 2015) and $\geq 5 \cdot 10^6 \text{ cells L}^{-1}$ for raphidophytes (Zhang et al., 2006)), were sorted and the frequency of bloom occurrence at each temperature was calculated. A total of 177, 113 and 59 bloom records were noted for *K. veneticum*, *H. akashiwo* and *C. subsalsa* respectively. These results were binned into six different temperature ranges (>10, 10–14, 15–19, 20–24, 25–29 and >30 °C respectively) and are shown in Fig. 4.

Across this sixteen year time-frame, *K. veneticum* bloom frequency increased with increasing temperature and tended to peak at 25–29 °C (53% of bloom total) and then decreased sharply to 9% at ≥ 30 °C. Similar to blooms in the Chesapeake Bay (Li et al., 2015), 71% of total *K. veneticum* blooms occurred when the water temperature was 20–29 °C. *H. akashiwo* did not bloom below 15 °C and 85% of blooms fell between 20 and 29 °C with bloom frequency peaking at 25–29 °C (57.5% of total) similar to *K. veneticum*. Comparable to our laboratory observations, all *C. subsalsa* blooms were noted at temperatures above 20 °C and *C. subsalsa* bloom occurrence was greater than *K. veneticum* and *H. akashiwo* (76%), at 25–29 °C. These historical observations agree with the thermal properties (*Topt*, thermal niche width and upper thermal boundaries) from our laboratory results with *K. veneticum* and *H. akashiwo*. While the in situ bloom data for *C. subsalsa* are not in complete agreement with regards to the laboratory growth patterns noted above 30 °C, this historical comparison suggests an association between temperature and bloom formation in the DIB.

A global analysis of growth TPC's from 194 strains of marine and estuarine phytoplankton suggested that *Topt* for phytoplankton growth in vitro is strongly related to the mean annual temperature for the location of isolation (Thomas et al., 2012), and a similar relationship was recently noted for eleven strains of the cyanobacteria *Micromonas* sp. (Demory et al., 2019). The three algal strains used in our study were originally isolated from the same geographic area and were maintained under the same laboratory conditions for several years. While the *Topt* patterns for *K. veneticum* and *H. akashiwo* agree with this trend, thermal growth patterns for *C. subsalsa* may also represent some phenotypic acclimation capacity as well as pre-existing, and *de novo* mutations in long-term laboratory culture conditions. Further, our results strongly suggest that such species-specific capacity for physiological acclimation to ocean warming could promote the growth and possibly bloom formation of *C. subsalsa*, especially when the temperature exceeds the thermal limits of other co-existing algal species.

4.2. Thermal response of PSII photochemistry

The photochemical responses to temperature where growth was positive were marked by three distinct trends across each algal species. Dark and light acclimated PSII photochemical efficiency (F_v/F_m and F_q'/F_m') remained stable in *K. veneficum*, while photochemistry in *H. akashiwo* and *C. subsalsa* was significantly affected by growth temperature, but in different ways. In particular, F_v/F_m and μ_{max} were closely correlated in *H. akashiwo* ($p < 0.03$, $R^2 = 0.84$), while *C. subsalsa* photochemical efficiency followed a more unimodal response that departed substantially from the more linear thermal growth response, with a steeper increase in F_v/F_m up to a T_{opt} at 25 °C and then a slower decline at temperatures above T_{opt} . It is not uncommon for some phytoplankton to maintain growth rate-independent PSII efficiency across a broad range of environmental stress, such as N-limitation (Halsey et al., 2010). In contrast, Baker et al. (2016) recently noted photochemical performance of the model diatom, *Thalassiosira pseudonana*, declined with increasing temperature and significantly departed from the thermal growth response which closely followed a bell-shaped curve. Similarly, other studies have noted both close correlations as well as departures between thermal performance trends in photochemistry vs. growth in several isolates of *Synechococcus* spp. (Mackey et al., 2013). On the other hand, heterotrophy (e.g., eating bacteria) may also have contributed to higher growth rates at temperatures above 25 °C, especially when PSII efficiency declined. While we did not measure mixotrophy or heterotrophy, others have noted that when growing at 20 °C, *C. subsalsa* maintains ingestion rates of up to 20.5 prey (*Synechococcus* sp.) cell⁻¹ h⁻¹ (Jeong et al., 2010). Furthermore, the metabolic contribution of heterotrophy in a mixotroph increases with the temperature (Wilken et al., 2013), which may also contribute to the significant departures between growth and photochemistry thermal performance patterns observed here.

Compared to previous work, our study approached a smaller temperature range (± 7 °C around the maintenance culture temperature of 25 °C), and thus further investigation at lower temperatures as well as greater granularity at higher temperatures (e.g., 30–32 °C) is needed to capture possibly greater differences in some photochemical traits for some algal species (e.g., *K. veneficum*) potentially driven by rate limitation of the dark or light reactions of photosynthesis at low and high temperatures, respectively (Baker et al., 2016). Nevertheless, the significant decline in dark and light acclimated PSII efficiency in *H. akashiwo* at 30 °C suggests that this alga may be more susceptible to high temperature limitations in the photosynthetic light reactions as compared to the other algal species. Meanwhile the significantly lower growth and photochemical response of *C. subsalsa* at 18 °C suggests a greater low-temperature sensitivity, which is also corroborated by its seasonal occurrence at higher temperatures in the DIB.

Phytoplankton also optimize physiology by modulating photosynthetic pigments in response to environmental parameters, such as light, nutrients, and temperature (Kruskopf and Flynn, 2011; Halsey et al., 2010; Cui et al., 2017). Notably, *K. veneficum* retained photochemical efficiency at 18 °C, while modulating light harvesting by low-temperature dependent adjustment of its PSII functional absorption cross section (σ_{PSII}). Cellular chl-*a* was quite variable in response to temperature in both raphidophyte species, but the significantly higher chl-*a* for *K. veneficum* at 18 °C is noteworthy. The concomitant increase in N cell quota and decrease of C:N in *K. veneficum* at 18 °C suggests a significant N investment in chlorophyll and light harvesting protein synthesis at 18 °C, while the decline in σ_{PSII} was likely a result of pigment packaging. Conversely the raphidophytes showed fewer adjustments in σ_{PSII} with temperature and are in agreement with the relatively constant σ_{PSII} noted in the diatom *Thalassiosira pseudonana* when grown over a 20 °C temperature gradient (Baker et al., 2016).

4.3. Temperature and species dependency of cell toxicity

Two trends emerged from our results on cell toxicity. First, the effect of temperature was species-specific such that *K. veneficum* toxicity was greatest at higher temperature (≥ 28 °C), while the raphidophytes' toxicity was the highest at 25–28 °C. Second, there were clear differences in the mode of toxicity between the dinoflagellate and the raphidophytes wherein *K. veneficum* had greater hemolytic activity than the raphidophyte, while fish gill toxicity was greater in the raphidophytes than for *K. veneficum*.

When growing autotrophically, increased cell toxicity is often associated with abiotic stress (Granéli and Flynn, 2006). As *K. veneficum* growth was beginning to decline at 30 °C, this temperature was potentially more stressful than sub-optimal temperatures (< 25 °C) or the elevated toxicity at higher temperature may represent a shift in cellular resource allocation. Cell volume can increase with temperature (Baker et al., 2016). While we did not measure cell volume directly, toxin activities were normalized to cellular carbon and hence (assuming that cellular C did not vary independently of cell volume) increased cell toxicity at higher temperature was due to increased toxin production and not merely a result of increased toxin accumulation. Therefore, temperatures up to ~28–29 °C may promote *K. veneficum* proliferation and induce higher toxin production. Conversely, the raphidophytes exhibited the highest toxicity at 25–28 °C, and any further temperature increase significantly reduced their toxicity. Therefore, toxicity in both raphidophytes seemed to be either optimized (*H. akashiwo*) or slightly sub-optimal (*C. subsalsa*) with regards to maximal growth. In contrast, Ikeda et al. (2016) noted that FGC toxicity by a different strain of *H. akashiwo* was neither temperature nor growth rate dependent.

Phytoplankton hemolytic activity may be linked to specific toxic compound(s). *K. veneficum* karlotoxins (KmTx-1 and KmTx-2) are highly hemolytic (Fu et al., 2010; Deeds et al., 2015), and while hemolytic activity noted here may be proportional to KmTx toxicity, direct quantification would be required to confirm this assertion. On the other hand, strong hemolytic activity produced by *Alexandrium tamarense* was not caused by its major toxic compounds; gonyautoxins (GTX₁₋₅) and saxitoxins (Simonsen et al., 1995). A more conservative view is that hemolytic activity is likely caused by a group of compounds rather than one major hemolytic agent. In fact, the presence of at least two other molecules, in addition to KmTx-1 and 2, with even stronger hemolytic activities have been reported for another strain of *K. veneficum* isolated from East China sea (Cai et al., 2016). Some fish-killing raphidophyte species (e.g. *Chattonella marina* and *C. Chattonella antiqua*) lack hemolytic activity while others have weak activity, which is expressed when the assay is performed under constant light (Cho et al., 2017). Similarly, *H. akashiwo* and *C. subsalsa* had significantly lower hemolytic activity compared to *K. veneficum* (Fig. 3) and was only expressed at constant light in this study. Such light-dependent hemolytic activity in raphidophytes may be linked to the presence of photosensitizing compounds (e.g. porphyrin derivatives) as major hemolytic compounds (Sato et al., 2002; Miyazaki et al., 2005). However, these hemolytic agents may not necessarily be the major toxins produced by raphidophytes.

In contrast to their low hemolytic activity, the two raphidophytes caused higher fish gill cell mortalities than *K. veneficum* (Fig. 3). This is similar to the results reported by Dorantes-Aranda et al., (2011). In some phytoplankton species (e.g. *Heterocapsa circularisquama*), both hemolytic activity and the cytotoxicity are attributed to the same photosensitizing hemolytic toxins (e.g. porphyrin derivatives) as they are only expressed in the light (Sato et al., 2002; Miyazaki et al., 2005; Wencheng et al., 2018). Unlike the hemolytic assay, we conducted the FGC assay in the dark yet found higher toxicities in raphidophytes. This suggests that raphidophyte toxins/noxious compounds that cause FGC mortality are different from their photosensitizing hemolytic agents. Extracellular exudates of some *H. akashiwo* strains can alter the metabolic activity of mammalian cell lines (Twiner et al., 2004). In addition,

some raphidophytes (e.g. *C. antiqua*) produce reactive oxygen species (ROS) which are also believed to damage fish gill cells (Zou et al., 2013). However, it is unlikely that ROS caused the FGC mortality in this present study, as only the activity of cell extracts and not intact cells were measured. While assessing the specific toxin compounds and their modes of action were beyond the scope of this work, further study is clearly warranted to differentiate the possible sources of toxicity among these species.

5. Conclusions

The results presented here are in agreement with previous studies (e.g. Hallegraeff, 2010; Wells et al., 2015; Gobler et al., 2017; Trainer et al., 2019) in that the expected outcomes of projected climate change, such as ocean warming, may promote the blooms of toxic HA species by directly increasing their growth and/or by widening the temporal window for bloom formation. These results provide valuable insight into the phenotypic plasticity of three major HAB species responds to ocean warming. Different functional traits exhibited different thermal performance and the *Topt* for growth does not necessarily reflect the *Topt* of underlying physiological traits. While these results do not fully represent the responses of in situ populations which are subjected to multifactorial control, this work suggests that (1) *K. veneficum* and *H. akashiwo* are perhaps already growing at temperatures close to their *Topt* in the DIB and elsewhere, and prolonged or earlier seasonal heating (near *Topt*) could widen their bloom window. (2) Ocean warming may promote highly toxic *K. veneficum* blooms thereby leading to significant negative environmental effects, and (3) because of its higher thermal limit for growth, *C. subsalsa* is quite resilient to warming and has the potential to bloom at temperatures that suppress the growth of other HAB species, yet its toxicity may not match such thermally-enhanced growth.

Declaration of Competing Interest

The authors declare that they have no known competing financial interests or personal relationships that could have appeared to influence the work reported in this paper.

Acknowledgments

We thank two anonymous reviewers for their valuable comments. We are grateful to Dr. Edward Whereat for sharing the data collected by the UD citizen phytoplankton monitoring program. This study was supported by the NOAA National Center for Coastal Ocean Science through grant NA15NOS4780182 awarded to M.E.W., KJC and JHC. This is contribution 960 to the ECOHAB program.

CG.

Supplementary materials

Supplementary material associated with this article can be found, in the online version, at [doi:10.1016/j.hal.2020.101804](https://doi.org/10.1016/j.hal.2020.101804).

References

- Adolf, J.E., Bachvaroff, T., Place, A.R., 2008. Can cryptophyte abundance trigger toxic *Karlotodinium veneficum* blooms in eutrophic estuaries? *Harmful Algae* 8, 119–128.
- Adolf, J.E., Bachvaroff, T.R., Deeds, J.R., Place, A.R., 2016. Ichthyotoxic *Karlotodinium veneficum* in the Upper Swan River Estuary (Western Australia): Synergistic Effects of Karlotoxin and Hypoxia Leading to a Fish Kill 83–93.
- Adolf, J.E., Bachvaroff, T.R., Place, A.R., 2009. Environmental modulation of *Karlotodinium veneficum* levels in strains of the cosmopolitan dinoflagellate, *Karlotodinium veneficum* (Dinophyceae). *J. Phycol.* 45, 176–192.
- Adolf, J.E., Krupatkin, D., Bachvaroff, T., Place, A.R., 2007. Karlotoxin mediates grazing by *Oxyrrhis marina* on strains of *Karlotodinium veneficum*. *Harmful Algae* 6, 400–412.
- Adolf, J.E., Stoecker, D.K., Harding, L.W., 2006. The balance of autotrophy and heterotrophy during mixotrophic growth of *Karlotodinium micrum* (Dinophyceae). *J. Plankton Res.* 28, 737–751.
- Anderson, D.M., Cembella, A.D., Hallegraeff, G.M., 2012. Progress in understanding harmful algal blooms: paradigm shifts and new technologies for research, monitoring, and management. *Ann. Rev. Mar. Sci.* 4, 143–176.
- Aquino-Cruz, A., Purdie, D.A., Morris, S., 2018. Effect of increasing sea water temperature on the growth and toxin production of the benthic dinoflagellate *Prorocentrum lima*. *Hydrobiologia* 813, 103–122.
- Bachvaroff, T.R., Adolf, J.E., Place, A.R., 2009. Strain variation in *Karlotodinium veneficum* (dinophyceae): toxin profiles, pigments, and growth characteristics. *J. Phycol.* 45, 137–153.
- Baker, K.G., Radford, D.T., Evenhuis, C., Kuzhumparam, U., Ralph, P.J., Doblin, M.A., 2018. Thermal niche evolution of functional traits in a tropical marine phototroph. *J. Phycol.* 54, 799–810.
- Baker, K.G., Robinson, C.M., Radford, D.T., McInnes, A.S., Evenhuis, C., Doblin, M.A., 2016. Thermal performance curves of functional traits aid understanding of thermally induced changes in diatom-mediated biogeochemical fluxes. *Front. Mar. Sci.* 3, 1–14.
- Basti, L., Suzuki, T., Uchida, H., Kamiyama, T., Nagai, S., 2018. Thermal acclimation affects growth and lipophilic toxin production in a strain of cosmopolitan harmful alga *Dinophysis acuminata*. *Harmful Algae* 73, 119–128.
- Baty, F., Ritz, C., Charles, S., Brutsche, M., Flandrois, J.-P., Delignette-Muller, M.-L., 2015. A toolbox for nonlinear regression in R: the package nlstools. *J. Stat. Softw.* 66, 1–21.
- Berdalet, E., Fleming, L.E., Gowen, R., Davidson, K., Hess, P., Backer, L.C., Moore, S.K., Hoagland, P., Enevoldsen, H., 2016. Marine harmful algal blooms, human health and wellbeing: challenges and opportunities in the 21st century. *J. Mar. Biol. Assoc. U. K.* 96, 61–91.
- Binzer, S.B., Lundgreen, R.B.C., Berge, T., Hansen, P.J., Vismann, B., 2018. The blue mussel *Mytilus edulis* is vulnerable to the toxic dinoflagellate *Karlotodinium armiger*—Adult filtration is inhibited and several life stages killed. *PLoS One* 13, 1–16.
- Boyd, P.W., Rynearson, T.A., Armstrong, E.A., Fu, F., Hayashi, K., Hu, Z., Hutchins, D.A., Kudela, R.M., Litchman, E., Mulholland, M.R., Passow, U., Strzepak, R.F., Whittaker, K.A., Yu, E., Thomas, M.K., 2013. Marine phytoplankton temperature versus growth responses from polar to tropical waters - Outcome of a scientific community-wide study. *PLoS One* 8, e63091. <https://doi.org/10.1371/journal.pone.0063091>.
- Brandenburg, K.M., Velthuis, M., Van De Waal, D.B., 2019. Meta-analysis reveals enhanced growth of marine harmful algae from temperate regions with warming and elevated CO₂ levels. *Glob. Change Biol.* 25, 2607–2618.
- Cai, P., He, S., Zhou, C., Place, A.R., Haq, S., Ding, L., Chen, H., Jiang, Y., Guo, C., Xu, Y., Zhang, J., Yan, X., 2016. Two new karlotoxins found in *Karlotodinium veneficum* (strain GM2) from the east china sea. *Harmful Algae* 58, 66–73.
- Cho, K., Kasaoka, T., Ueno, M., Basti, L., Yamasaki, Y., Kim, D., Oda, T., 2017. Haemolytic activity and reactive oxygen species production of four harmful algal bloom species. *Eur. J. Phycol.* 52, 311–319.
- Cho, K., Sakamoto, J., Noda, T., Nishiguchi, T., Ueno, M., Yamasaki, Y., Yagi, M., Kim, D., Oda, T., 2016. Comparative studies on the fish-killing activities of *Chattonella marina* isolated in 1985 and *Chattonella antiqua* isolated in 2010, and their possible toxic factors. *Biosci. Biotechnol. Biochem.* 80, 811–817.
- Cosgrove, J., Borowitzka, M.A., 2010. Chlorophyll fluorescence terminology: an introduction. In: Suggett, D.J., Prášil, O., Borowitzka, M.A. (Eds.), *Chlorophyll a Fluorescence in Aquatic Sciences: Methods and Applications*. Springer, Netherlands, Dordrecht, pp. 1–17.
- Coyne, K.J., Handy, S.M., Demir, E., Whereat, E.B., Hutchins, D.A., Portune, K.J., Doblin, M.A., Cary, S.C., 2005. Improved quantitative real-time pcr assays for enumeration of harmful algal species in field samples using an exogenous dna reference standard. *Limnol. Oceanogr. Methods* 3, 381–391.
- Cui, Y., Zhang, H., Lin, S., 2017. Enhancement of non-photochemical quenching as an adaptive strategy under phosphorus deprivation in the dinoflagellate *Karlotodinium veneficum*. *Front. Microbiol.* 8, 1–14.
- Dayeh, V.R., Schirmer, K., Lee, L.E.J., Bols, N.C., 2005. Rainbow trout gill cell line microplate cytotoxicity test. In: Blaise, C., Féraud, J.-F. (Eds.), *Small-Scale Freshwater Toxicity Investigations: Toxicity Test Methods*. Springer, Netherlands, Dordrecht, pp. 473–503.
- de Boer, M.K., Boerée, C., Sjollem, S.B., de Vries, T., Rijnsdorp, A.D., Buma, A.G.J., 2012. The toxic effect of the marine raphidophyte *Fibrocapsa japonica* on larvae of the common flatfish sole (*Solea solea*). *Harmful Algae* 17, 92–101.
- Deeds, J.R., Hoesch, R.E., Place, A.R., Kao, J.P.Y., 2015. The cytotoxic mechanism of karlotoxin 2 (KmTx 2) from *Karlotodinium veneficum* (Dinophyceae). *Aquat. Toxicol.* 159, 148–155.
- Deeds, J.R., Terlizzi, D.E., Adolf, J.E., Stoecker, D.K., Place, A.R., 2002. Toxic activity from cultures of *Karlotodinium micrum* (= *Gyrodinium galatheanum*) (Dinophyceae) - A dinoflagellate associated with fish mortalities in an estuarine aquaculture facility. *Harmful Algae* 1, 169–189.
- Demir, E., Coyne, K.J., Doblin, M.A., Handy, S.M., Hutchins, D.A., 2008. Assessment of microzooplankton grazing on *Heterosigma akashiwo* using a Species-Specific Approach combining quantitative real-time pcr (QPCR) and dilution methods. *Microb. Ecol.* 55, 583–594.
- Demory, D., Baudoux, A.C., Monier, A., Simon, N., Six, C., Ge, P., Rigaut-Jalabert, F., Marie, D., Sciandra, A., Bernard, O., Rabouille, S., 2019. Picoeukaryotes of the *Micromonas* genus: sentinels of a warming ocean. *ISME J.* 13, 132–146.
- Dorantes-Aranda, J.J., Waite, T.D., Godrant, A., Rose, A.L., Tovar, C.D., Woods, G.M., Hallegraeff, G.M., 2011. Novel application of a fish gill cell line assay to assess ichthyotoxicity of harmful marine microalgae. *Harmful Algae* 10, 366–373.
- Eschbach, E., Scharsack, J.P., John, U., Medlin, L.K., 2001. Improved erythrocyte lysis assay in microtitre plates for sensitive detection and efficient measurement of haemolytic compounds from ichthyotoxic algae. *J. Appl. Toxicol.* 21, 513–519.

- Falkowski, P.G., Barber, R.T., Smetacek, V., 1998. Biogeochemical controls and feedbacks on ocean primary production. *Science* (80-) 281 LP-206.
- Field, C.B., Behrenfeld, M.J., Randerson, J.T., Falkowski, P., 1998. Primary production of the biosphere: integrating terrestrial and oceanic components. *Science* (80-) 281 237 LP-240.
- Fredrickson, K.A., Strom, S.L., Crim, R., Coyne, K.J., 2011. Interstrain variability in physiology and genetics of *Heterosigma akashiwo* (Raphidophyceae) from the west coast of north america. *J. Phycol.* 47, 25–35.
- Fu, F.X., Place, A.R., Garcia, N.S., Hutchins, D.A., 2010. CO₂ and phosphate availability control the toxicity of the harmful bloom dinoflagellate *Karlodinium veneficum*. *Aquat. Microb. Ecol.* 59, 55–65.
- Fu, F.X., Zhang, Y., Warner, M.E., Feng, Y., Sun, J., Hutchins, D.A., 2008. A comparison of future increased CO₂ and temperature effects on sympatric *Heterosigma akashiwo* and *Prorocentrum minimum*. *Harmful Algae* 7, 76–90.
- Geider, R.J., Moore, C.M., Rosco, O.N., 2009. The role of cost-benefit analysis in models of phytoplankton growth and acclimation. *Plant Ecol. Divers.* 2, 165–178.
- Glibert, P.M., 2016. Margalef revisited: a new phytoplankton mandala incorporating twelve dimensions, including nutritional physiology. *Harmful Algae* 55, 25–30.
- Gobler, C.J., Doherty, O.M., Hattenrath-Lehmann, T.K., Griffith, A.W., Kang, Y., Litaker, R.W., 2017. Ocean warming since 1982 has expanded the niche of toxic algal blooms in the north atlantic and north pacific oceans. *Proc. Natl. Acad. Sci.* 114, 4975–4980.
- Granéli, E., Flynn, K., 2006. Chemical and physical factors influencing toxin content. In: Granéli, Edna, Turner, J.T. (Eds.), *Ecology of Harmful Algae*. Springer, Berlin, Heidelberg, pp. 229–241.
- Granéli, E., Vidyarthna, N.K., Funari, E., Cumararatunga, P.R.T., Scenati, R., 2011. Can increases in temperature stimulate blooms of the toxic benthic dinoflagellate *Ostreopsis ovata*? *Harmful Algae* 10, 165–172.
- Guillard, R.R.L., Ryther, J.H., 1962. Studies of marine planktonic diatoms: I. *Cyclotella nana* hustedt, and *Detonula confervacea* (Cleve) gran. *Can. J. Microbiol.* 8, 229–239.
- Hallegraeff, G.M., 2010. Ocean climate change, phytoplankton community responses, and harmful algal blooms: a formidable predictive challenge. *J. Phycol.* 46, 220–235.
- Halsey, K.H., Milligan, A.J., Behrenfeld, M.J., 2010. Physiological optimization underlies growth rate-independent chlorophyll-specific gross and net primary production. *Photosynth. Res.* 103, 125–137.
- Handy, S.M., Coyne, K.J., Portune, K.J., Demir, E., Doblin, M.A., Hare, C.E., Cary, S.C., Hutchins, D.A., 2005. Evaluating vertical migration behavior of harmful raphidophytes in the delaware inland bays utilizing quantitative real-time pcr. *Aquat. Microb. Ecol.* 40, 121–132.
- Handy, S.M., Demir, E., Hutchins, D.A., Portune, K.J., Whereat, E.B., Hare, C.E., Rose, J.M., Warner, M., Farestad, M., Cary, S.C., Coyne, K.J., 2008. Using quantitative real-time pcr to study competition and community dynamics among delaware inland bays harmful algae in field and laboratory studies. *Harmful Algae* 7, 599–613.
- Hennige, S.J., Coyne, K.J., Macintyre, H., Liefer, J., Warner, M.E., 2013. The photobiology of *Heterosigma akashiwo*. photoacclimation, diurnal periodicity, and its ability to rapidly exploit exposure to high light. *J. Phycol.* 49, 349–360.
- Ikedo, C.E., Cochlan, W.P., Bronicheski, C.M., Trainer, V.L., Trick, C.G., 2016. The effects of salinity on the cellular permeability and cytotoxicity of *Heterosigma akashiwo*. *J. Phycol.* 52, 745–760.
- Imai, I., Yamaguchi, M., 2012. Life cycle, physiology, ecology and red tide occurrences of the fish-killing raphidophyte *Chattonella*. *Harmful Algae* 14, 46–70.
- IPCC, 2013. IPCC Fifth Assess. Rep. IPCC, pp. 1–29.
- Jeong, H.J., Seong, K.A., Kang, N.S., Yoo, Y., Du, Nam, S.W., Park, J.Y., Shin, W., Glibert, P.M., Johns, D., 2010. Feeding by raphidophytes on the cyanobacterium. *Aquat. Microb. Ecol.* 58, 181–195.
- Kibler, S.R., Litaker, R.W., Holland, W.C., Vandersea, M.W., Tester, P.A., 2012. Growth of eight *Gambierdiscus* (Dinophyceae) species: effects of temperature, salinity and irradiance. *Harmful Algae* 19, 1–14.
- Kruskopf, M., Flynn, K.J., 2011. Chlorophyll content and fluorescence responses chlorophyll content to gauge used reliably phytoplankton status or cannot nutrient be growth rate. *New Phytol.* 169, 525–536.
- Li, J., Glibert, P.M., Gao, Y., 2015. Temporal and spatial changes in chesapeake bay water quality and relationships to *Prorocentrum minimum*, *Karlodinium veneficum*, and cyanobab events, 1991–2008. *Harmful Algae* 42, 1–14.
- Lin, C.-H., Flynn, K.J., Mitra, A., Glibert, P.M., 2018a. Simulating effects of variable stoichiometry and temperature on mixotrophy in the harmful dinoflagellate *Karlodinium veneficum*. *Front. Mar. Sci.* 5, 1–13.
- Lin, C.H.(Michelle), Lyubchich, V., Glibert, P.M., 2018b. Time series models of decadal trends in the harmful algal species *Karlodinium veneficum* in chesapeake bay. *Harmful Algae* 73, 110–118.
- Lin, C.H., Accoroni, S., Glibert, P.M., 2017. *Karlodinium veneficum* feeding responses and effects on larvae of the eastern oyster *Crassostrea virginica* under variable nitrogen:phosphorus stoichiometry. *Aquat. Microb. Ecol.* 79, 101–114.
- Litchman, E., de Tezanos Pinto, P., Edwards, K.F., Klausmeier, C.A., Kremer, C.T., Thomas, M.K., 2015. Global biogeochemical impacts of phytoplankton: a trait-based perspective. *J. Ecol.* 103, 1384–1396.
- Litchman, E., Edwards, K.F., Klausmeier, C.A., Thomas, M.K., 2012. Phytoplankton niches, traits and eco-evolutionary responses to global environmental change. *Mar. Ecol. Prog. Ser.* 470, 235–248.
- Mackey, K.R.M., Paytan, A., Caldeira, K., Grossman, A.R., Moran, D., McIlvin, M., Saito, M.A., 2013. Effect of temperature on photosynthesis and growth in marine *Synechococcus* spp. *Plant Physiol.* 163, 815–829.
- Martínez, R., Orive, E., Laza-Martínez, A., Seoane, S., 2010. Growth response of six strains of *Heterosigma akashiwo* to varying temperature, salinity and irradiance conditions. *J. Plankton Res.* 32, 529–538.
- Miyazaki, Y., Nakashima, T., Iwashita, T., Fujita, T., Yamaguchi, K., Oda, T., 2005. Purification and characterization of photosensitizing hemolytic toxin from harmful red tide phytoplankton, *Heterosigma circularisquama*. *Aquat. Toxicol.* 73, 382–393.
- Mooney, B.D., Hallegraeff, G.M., Place, A.R., 2010. Ichthyotoxicity of four species of gymnodinoid dinoflagellates (Kareniaceae, dinophyta) and purified karlotoxins to larval sheepshead minnow. *Harmful Algae* 9, 557–562.
- Moore, S.K., Trainer, V.L., Mantua, N.J., Parker, M.S., Laws, E.A., Backer, L.C., Fleming, L.E., Mantua, N.J., Parker, M.S., Laws, E.A., 2008. Impacts of climate variability and future climate change on harmful algal blooms and human health. *Environ. Health* 7 (Suppl 2), S4.
- Nedwell, D.B., 1999. Effect of low temperature on microbial growth: lowered affinity for substrates limits growth at low temperature. *FEMS Microbiol. Ecol.* 30, 101–111.
- Nielsen, M.V., 1996. Growth and chemical composition of the toxic dinoflagellate *Gymnodinium galatheanum* in relation to irradiance, temperature and salinity. *Mar. Ecol. Prog. Ser.* 136, 205–211.
- Ou, G., Wang, H., Si, R., Guan, W., 2017. The dinoflagellate *Akashiwo sanguinea* will benefit from future climate change: the interactive effects of ocean acidification, warming and high irradiance on photophysiology and hemolytic activity. *Harmful Algae* 68, 118–127.
- Padfield, D., Matheson, G., 2018. nls.multstart: Robust Non-Linear Regression Using Aic Scores. R package version 1.0.0. 1–5.
- Paerl, H.W., Huisman, J., 2009. Climate change: a catalyst for global expansion of harmful cyanobacterial blooms. *Environ. Microbiol. Rep.* 1, 27–37.
- Place, A.R., Bowers, H.A., Bachvaroff, T.R., Adolf, J.E., Deeds, J.R., Sheng, J., 2012. *Karlodinium veneficum*-The little dinoflagellate with a big bite. *Harmful Algae* 14, 179–195.
- Portune, K.J., Coyne, K.J., Hutchins, D.A., Handy, S.M., Cary, S.C., 2009. Quantitative real-time pcr for detecting germination of *Heterosigma akashiwo* and *Chattonella subsalsa* cysts from delaware's inland bays, usa. *Aquat. Microb. Ecol.* 55, 229–239.
- Portune, K.J., Craig Cary, S., Warner, M.E., 2010. Antioxidant enzyme response and reactive oxygen species production in marine raphidophytes. *J. Phycol.* 46, 1161–1171.
- RAVEN, J.A., GEIDER, R.J., 1988. Temperature and algal growth. *New Phytol.* 110, 441–461.
- Salvucci, M.E., Crafts-Brandner, S.J., 2004. Relationship between the heat tolerance of photosynthesis and the thermal stability of rubisco activase in plants from contrasting thermal environments. *Plant Physiol.* 134 1460 LP-1470.
- Sato, Y., Oda, T., Muramatsu, T., Matsuyama, Y., Honjo, T., 2002. Photosensitizing hemolytic toxin in *Heterosigma circularisquama*, a newly identified harmful red tide dinoflagellate. *Aquat. Toxicol.* 56, 191–196.
- Schirmer, K., Chan, A.G.J., Greenberg, B.M., Dixon, D.G., Bols, N.C., 1997. Methodology for demonstrating and measuring the photocytotoxicity of fluoranthene to fish cells in culture. *Toxicol. In Vitro* 11, 107–113.
- Schoofield, R.M., Sharpe, P.J., Magnuson, C.E., 1981. Non-linear regression of biological temperature-dependent rate models based on absolute reaction-rate theory. *J. Theor. Biol.* 88, 719.
- Shikata, T., Nagasoe, S., Matsubara, T., Yamasaki, Y., Shimasaki, Y., Oshima, Y., Honjo, T., 2007. Effects of Temperature and Light on Cyst Germination and Germinated Cell Survival of the Noxious Raphidophyte *Heterosigma Akashiwo*6, 700–706.
- Shikata, T., Nagasoe, S., Matsubara, T., Yoshikawa, S., Yamasaki, Y., Shimasaki, Y., Oshima, Y., Jenkinson, I.R., Honjo, T., 2008. Factors influencing the initiation of blooms of the raphidophyte *Heterosigma akashiwo* and the diatom *Skeletonema costatum* in a port in Japan. *Limnol. Oceanogr.* 53, 2503–2518.
- Simonsen, S., Moeller, B.L., Larsen, J., Ravn, H., Lassus, P., Moller, B.L., Larsen, J., Ravn, H., 1995. Haemolytic activity of *Alexandrium tamarense* cells. In: Lassus, Q., Arzul, G., Erard-Le-Denn, E., Gentien, Q. (Eds.), *Harmful Marine Algal Blooms. #Proliferation D' Algues Marines Nuisibles*. Lavoisier, Paris, pp. 513–517.
- Stawiariski, B., Buitenhuis, E.T., Le Quéré, C., 2016. The physiological response of pico-phytoplankton to temperature and its model representation. *Front. Mar. Sci.* 3, 1–13.
- Strom, S.L., Harvey, E.L., Fredrickson, K.A., Menden-Deuer, S., 2013. Broad salinity tolerance as a refuge from predation in the harmful raphidophyte alga *Heterosigma akashiwo* (Raphidophyceae). *J. Phycol.* 49, 20–31.
- Tester, P.A., Feldman, R.L., Nau, A.W., Kibler, S.R., Wayne Litaker, R., 2010. Ciguatera fish poisoning and sea surface temperatures in the caribbean sea and the west indies. *Toxicol.* 56, 698–710.
- Thomas, M.K., Kremer, C.T., Klausmeier, C.A., Litchman, E., 2012. A global pattern of thermal adaptation in marine phytoplankton. *Science* 338, 1085–1088 (80-).h.
- Tillmann, U., John, U., 2002. Toxic effects of *Alexandrium* spp. on heterotrophic dinoflagellates: an allelochemical defence mechanism independent of PSP-toxin content. *Mar. Ecol. Prog. Ser.* 230, 47–58.
- Tilney, C.L., Pokrzywinski, K.L., Coyne, K.J., Warner, M.E., 2014. Growth, death, and photobiology of dinoflagellates (Dinophyceae) under bacterial-algicide control. *J. Appl. Phycol.* 26, 2117–2127.
- Trainer, V.L., Moore, S.K., Hallegraeff, G., Kudela, R.M., Clement, A., Mardones, J.I., Cochlan, W.P., 2019. Pelagic harmful algal blooms and climate change: lessons from nature's experiments with extremes. *Harmful Algae* 91, 1–14.
- Twiner, M.J., Dixon, S.J., Trick, C.G., 2004. Extracellular organics from specific cultures of *Heterosigma akashiwo* (Raphidophyceae) irreversibly alter respiratory activity in mammalian cells. *Harmful Algae* 3, 173–182.
- Vidyarthna, N.K., Granéli, E., 2012. Influence of Temperature on Growth, Toxicity and Carbohydrate Production of a Japanese *Ostreopsis Ovata* Strain. A Toxic-Bloom-Forming Dinoflagellate65, 261–270.
- Waggett, R.J., Tester, P.A., Place, A.R., 2008. Anti-grazing properties of the toxic dinoflagellate *Karlodinium veneficum* during predator-prey interactions with the copepod *Acartia tonsa*. *Mar. Ecol. Prog. Ser.* 366, 31–42.
- Wells, Mark L, Trainer, V.L., Smayda, T.J., Karlson, B.S.O., Trick, C.G., Kudela, R.M., Ishikawa, A., Bernard, S., Wulff, A., Anderson, D.M., Cochlan, W.P., 2015. Harmful algal blooms and climate change: learning from the past and present to forecast the future. *Harmful Algae* 49, 68–93.

- Welschmeyer, N.A., 1994. Fluorometric analysis of chlorophyll a in the presence of chlorophyll b and pheopigments. *Limnol. Oceanogr.* 39, 1985–1992.
- Wencheng, L., Cho, K., Yamasaki, Y., Takeshita, S., Hwang, K., Kim, D., Oda, T., 2018. Photo-induced antibacterial activity of a porphyrin derivative isolated from the harmful dinoflagellate *Heterocapsa circularisquama*. *Aquat. Toxicol.* 201, 119–128.
- Wickham, H., 2019. **modelr: Modelling Functions That Work with the Pipe, Version 0.1.5.**
- Wilken, S., Huisman, J., Naus-Wiezer, S., Van Donk, E., 2013. Mixotrophic organisms become more heterotrophic with rising temperature. *Ecol. Lett.* 16, 225–233.
- Yamaguchi, H., Mizushima, K., Sakamoto, S., Yamaguchi, M., 2010. Effects of temperature, salinity and irradiance on growth of the novel red tide flagellate *Chattonella ovata* (Raphidophyceae). *Harmful Algae* 9, 398–401.
- Zhang, Y., Fu, F.X., Whereat, E., Coyne, K.J., Hutchins, D.A., 2006. Bottom-up controls on a mixed-species hab assemblage: a comparison of sympatric *Chattonella subsalsa* and *Heterosigma akashiwo* (Raphidophyceae) isolates from the Delaware Inland Bays, USA. *Harmful Algae* 5, 310–320.
- Zhou, C., Fernández, N., Chen, H., You, Y., Yan, X., 2011. Toxicological studies of *Karlodinium micrum* (Dinophyceae) isolated from East China Sea. *Toxicon* 57, 9–18.
- Zou, Y., Kim, D., Yagi, M., Yamasaki, Y., Kurita, J., Iida, T., Matsuyama, Y., Yamaguchi, K., Oda, T., 2013. Application of LDH-release assay to cellular-level evaluation of the toxic potential of harmful algal species. *Biosci. Biotechnol. Biochem.* 77, 345–352.